Calmodulin Binding to the C-Terminus of the Small-Conductance Ca^{2+}-Activated K^+ Channel hSK1 Is Affected by Alternative Splicing†

Bing-Mei Zhang,‡,§ Vipin Kohli,‡,§ Roberto Adachi,‡,§ José A. López,‡,§,|| Mark M. Udden,‡ and Richard Sullivan*,‡,§,⊥

Departments of Medicine, Molecular Physiology and Biophysics, and Molecular Genetics, Baylor College of Medicine, and Research Department, VA Medical Center, Houston, Texas 77030

Received July 19, 2000; Revised Manuscript Received December 27, 2000

ABSTRACT: We identified three splice variants of hSK1 whose C-terminal structures are determined by the independent deletion of two contiguous nucleotide sequences. The upstream sequence extends 25 bases in length, is initiated by a donor splice site within exon 8, and terminates at the end of the exon. The downstream sequence consists of nine bases that compose exon 9. When the upstream sequence ($hSK1^{-25b}$) or both sequences ($hSK1^{-34b}$) are deleted, truncated proteins are encoded in which the terminal 118 amino acids are absent. The binding of calmodulin to these variants is diminished, particularly in the absence of Ca^{2+} ions. The first 20 amino acids of the segment deleted from $hSK1^{-25b}$ and $hSK1^{-34b}$ contain a 1−8−14 Ca^{2+}-calmodulin binding motif, and synthetic oligopeptides based on this region bind calmodulin better in the presence than absence of Ca^{2+} ions. When the downstream sequence ($hSK1^{-9b}$) alone is deleted, only the three amino acids A452, Q453, and K454 are removed, and calmodulin binding is not reduced. On the basis of the relative abundance of mRNA encoding each of the four isoforms, the full-length variant appears to account for most hSK1 in the human hippocampus, while $hSK1^{-34b}$ predominates in reticulocytes, and $hSK1^{-9b}$ is especially abundant in human erythroleukemia cells in culture. We conclude that the binding of calmodulin by hSK1 can be modulated through alternative splicing.

Ca^{2+}-activated K^+ channels have traditionally been categorized on the basis of their single-channel conductances as either "big" (BK channels, ∼100−250 pS), "intermediate" (IK channels, ∼20−50 pS), or "small" (SK channels, ∼5−15 pS). Although it is clear that BK channels constitute a distinct K^+ channel family (*Slo* or BK family) (*1*), the close structural similarities of IK and SK channels that have recently come to light make it appropriate to classify these channels together (SK/IK family) (*2*−*5*). BK channels, which are both Ca^{2+}- and voltage-dependent, are assembled from pore-forming α-subunits encoded by the *Slo* gene (*1*). SK/IK channels, which are insensitive to voltage and gated primarily by fluctuations in the cytosolic concentration of Ca^{2+} ions ($[Ca^{2+}]i$), derive their pore-forming subunits from a family of four closely related genes (SK1, SK2, SK3, and IK1) (*2*−*5*). BK and SK/IK channels differ significantly not only in structure and electrophysiological behavior but also in their mechanisms of gating by Ca^{2+} ions. BK channels, which require relatively large increases in $[Ca^{2+}]i$ to increase their open state probability, contain a highly conserved putative Ca^{2+}-binding domain near the end of their C-terminal cytoplasmic tail (*1*) that may or may not (*6*) be the sole mechanism through which gating by Ca^{2+} ions occurs. However, in SK/IK channels, which are exquisitely sensitive to small elevations in $[Ca^{2+}]i$, Ca^{2+}-binding motifs are conspicuously absent (*7*, *8*). In these channels, calmodulin has recently been shown to bind to the cytoplasmic C-terminus and is thought to function as a modulatory subunit through which $[Ca^{2+}]i$ elevation is coupled to channel opening (*7*−*10*). As a result of these reports, the concept has developed that Ca^{2+} ions gate SK/IK channels by binding not directly to the pore-forming subunits but instead to calmodulin constitutively bound to the channel.

The volume of the red blood cell is controlled in part by voltage-independent Ca^{2+}-activated K^+ channels that are thought to number no more than 10 per cell (*11*, *12*). Several laboratories have isolated these channels either in cell-free, inside-out membrane patches (*11*, *13*−*15*) or in cell-attached patches (*11*) and recorded their single-channel conductances. The surprisingly wide variation of unitary conductances reported for these channels, which have ranged from 13.5 pS (*13*) to 75 pS (*15*), led us to consider the possibility that red cells may express more than one type of SK/IK channel.

In support of this view, we found that isolated human reticulocytes and cells from the human erythroleukemia lines *HEL* and *Dami* contain mRNA that codes for both the intermediate conductance Ca^{2+}-activated K^+ (IK)[1] channel hIK1[2] and the small conductance Ca^{2+}-activated K^+ (SK) channel hSK1. By means of the reverse transcriptase−polymerase chain reaction (RT-PCR), we identified a single

† This research was supported by the Research Service of the Department of Veterans' Affairs (Merit Review) and by the National Institutes of Health (HL 54218).

* Address correspondence to this author at mail stop 111H, Houston VA Medical Center, 2002 Holcombe, Houston, TX 77030. E-mail: freds@bcm.tmc.edu. Tel: 713 794-7111. Fax: 713 794-7733.

‡ Department of Medicine, Baylor College of Medicine.

§ Research Department, VA Medical Center.

|| Department of Molecular Genetics, Baylor College of Medicine.

⊥ Department of Molecular Physiology and Biophysics, Baylor College of Medicine.

10.1021/bi001675h CCC: $20.00
Published on Web 02/15/2001

form of hIK1 from these cells, which was identical in its entire coding region to that present in pancreas (hIK1) (*2*), lymphocytes (hKCa4) (*4*), and brain (hSK4) (*3*). In contrast to the single species of hIK1, we found four separate isoforms of hSK1 whose structures were determined by the independent inclusion or deletion of two adjacent nucleotide sequences within the region encoding the C-terminal cytoplasmic tail. The full-length isoform, which appears to be the predominant form of hSK1 in the human hippocampus, accounts for a much smaller fraction of hSK1 expressed in erythroid cells.

In reticulocytes, the major species of hSK1 appears to be a truncated variant ($hSK1^{-34b}$) in which half of the C-terminal cytoplasmic domain is deleted. Calmodulin binding in the absence of Ca^{2+} ions (apocalmodulin binding) to the C-terminus of $hSK1^{-34b}$ is markedly reduced when compared to hSK1. In a second truncated variant, $hSK1^{-25b}$, which is less abundantly expressed in erythroid cells, apocalmodulin binding is similarly impaired. In both $hSK1^{-25b}$ and $hSK1^{-34b}$, the C-terminal truncation transects a region that has been found to be important for calmodulin binding in the closely related channels rSK2 (*7*, *9*) and hIK1 (*10*), both in the presence (Ca^{2+}-calmodulin binding) as well as absence of Ca^{2+} ions. The first 20 amino acids of the deleted C-terminal fragment contain a 1−8−14 Ca^{2+}-calmodulin (*16*) binding motif as well as two positively charged amino acids (R456 and K459) determined by Keen et al. (*9*) to be critical for apocalmodulin binding. We found that a synthetic peptide containing these 20 residues exhibited both apocalmodulin and Ca^{2+}-calmodulin binding properties, although binding of calmodulin was clearly enhanced by Ca^{2+} ions.

In the leukemic cell line *Dami*, which is growth factor-independent and highly proliferative, an isoform in which only the three amino acids A452, Q453, and K454 are deleted ($hSK1^{-9b}$) is much more highly expressed than in either human hippocampus or reticulocytes. Although the 1−8−14 motif is disrupted in this variant, neither Ca^{2+}-calmodulin nor apocalmodulin binding is apparently altered. At present, the effects that this deletion exerts on the function of hSK1 are unclear. Taken together, the findings that we report lead us to predict that variations in the structure of hSK1 arising from posttranscriptional modification of its C-terminal sequence may equip the channel for particular functions in different tissues by altering its gating by calmodulin.

EXPERIMENTAL PROCEDURES

Cells. Peripheral blood samples were obtained from patients with sickle cell disease following guidelines approved by the Institutional Review Board for Human Experimentation of Baylor College of Medicine. Platelet-rich plasma was removed by low-speed centrifugation. The red cell-rich fraction was washed with Tris-buffered saline and then filtered through a column containing α-cellulose and methylcellulose as described by Beutler et al. (*17*). The cells were then suspended in cell-free plasma and separated on a density gradient (*18*). The buoyant reticulocyte-rich preparation was removed and used for isolation of RNA. The human erythroleukemia (*HEL*) cell line and its closely related subline *Dami* were obtained from the American Type Culture Collection (Rockville, MD). The cells were grown in RPMI 1640 medium containing 10% fetal calf serum and supplemented with penicillin and streptomycin as previously described (*19*).

Reverse Transcriptase−Polymerase Chain Reaction (RT-PCR). Following cellular lysis in guanidine isothiocyanate, RNA was isolated from reticulocytes or from cells of the human leukemia lines *HEL* and *Dami* by ultraspeed centrifugation on cesium chloride gradients. mRNA was prepared from *Dami* cell RNA using the Oligotex mRNA Mini Kit (Qiagen, Chatsworth, CA). mRNA from the hippocampus of human brain (poly A^+ RNA) was purchased from Clontech (Palo Alto, CA). Reverse transcription was then performed in each experiment using the GeneAmp Kit (Perkin-Elmer, Foster City, CA). cDNA was subsequently amplified by hot-start PCR with Taq polymerase in the presence of Q-solution (Qiagen).

Amplification and Cloning of the Four hSK1 Isoforms. The oligonucleotide primers hSK1-del sense and hSK1-del α-sense, which span 166 bases in the full-length isoform of hSK1 and encompass the two deletion fragments, were designed to amplify the pertinent region of each of the four isoforms. RT-PCR was carried out with these primers using hippocampal or *Dami* mRNA as template. The total RT-PCR products were purified by gel extraction and cloned in the plasmid vector PCR 2.1 (Invitrogen, Carlsbad, CA). The plasmid DNA was then sequenced in order to identify each of the four isoforms.

Nested PCR was done to resolve each of the four isoforms from reticulocyte RNA. The primers hSK1-RPA-sense and hSK1-del α-sense were used for initial amplification, and hSK1-del sense and hSK1-del α-sense were subsequently used to visualize a more restricted region encompassing the deletions.

Genomic Cloning. Genomic DNA was purified from *Dami* cells using the DNeasy Tissue Kit (Qiagen). PCR was then carried out using the oligonucleotide primers hSK1-del sense and hSK1-del α-sense to amplify the region of interest. The PCR product was cloned in the plasmid vector PCR 2.1 (Invitrogen) and sequenced using a panel of oligonucleotide primers. The final sequence was then aligned according to the published genomic sequence of hSK1 [KCNN1 (*20*) (GenBank Accession Number 6631091)] and found to correspond to a region between exons 8 and 10.

Ribonuclease Protection Assay. A fragment of DNA that extended from the 1267th to the 1432nd base of the coding region of hSK1 was amplified by RT-PCR from human hippocampal mRNA using the oligonucleotides hSK1-del sense and hSK1-del α-sense. Following cloning in the plasmid vector PCR 2.1 (Invitrogen), the plasmid DNA was linearized with *Hin*dIII, purified, and used to synthesize a riboprobe in the presence of ^{33}P-labeled nucleotides (MAXIscript In Vitro Transcription Kit, Ambion, Austin, TX). After the riboprobe was hybridized with mRNA overnight at 42

[1] Abbreviations: BK, large ("big") conductance Ca^{2+}-activated K^+ channel; $[Ca^{2+}]i$, cytosolic concentration of Ca^{2+} ions; EGTA, ethylene glycol bis(β-aminoethyl ether)-*N*,*N*,*N*′,*N*′-tetraacetic acid; GST, glutathione *S*-transferase; HEL, human erythroleukemia cell line; IK, intermediate conductance Ca^{2+}-activated K^+ channel; PCR, polymerase chain reaction; RT-PCR, reverse transcriptase−polymerase chain reaction; SK, small conductance Ca^{2+}-activated K^+ channel; SDS, sodium dodecyl sulfate.

[2] This channel was named hIK1 (*2*), hKCa4 (*4*), and hSK4 (*3*) by the independent laboratories that identified it simultaneously. We refer to this channel as hIK1 throughout this paper.

Table 1: Synthetic Peptides

peptide sequence[a]	isoform
ARVRKHQRKFLQAIHQAQKLRSVKIEQG	hSK1
ARVRKHQRKFLQAIHQLRSVKIEQG	hSK1^{-9b}
ARVRKHQRSGV	hSK1^{-34b}

[a] Corresponds to the sequence extending from A436 of the C-terminus.

°C, the RNA complexes were digested with RNases (RPA II kit, Ambion). The samples were electrophoresed on 5% polyacrylamide gels containing 8 M urea and then were developed by autoradiography. A β-actin riboprobe was used to confirm equal loading of RNA, and total yeast RNA was used as a negative control.

Calmodulin Binding Studies. Fusion proteins were synthesized in which glutathione *S*-transferase (GST) was linked to the cytosolic C-terminus of each of the four hSK1 splice variants. RT-PCR was first performed to amplify DNA sequences encoding each of the isoforms beginning with the codon for K386 and extending to the end of the coding frame. The primers hSK1-CTERM sense and hSK1-CTERM α-sense that were used for amplification were constructed to add an *Eco*RI restriction site onto the upstream end and a *Xho*I site onto the downstream end of each sequence. Following initial cloning in PCR 2.1, the inserts were subcloned in the vector pGEX-5X-1 (Amersham Pharmacia Biotech, Piscataway, NJ), which contained the GST coding region. Transformation was carried out using *Escherichia coli* BL21 (Amersham Pharmacia Biotech). The synthesis of each GST fusion protein was induced with isopropyl β-D-thiogalactoside. The fusion proteins were harvested and adsorbed to Sepharose beads as previously described (*21*). Each sample of beads (~100 μL) was washed and resuspended in 600 μL of Tris-buffered saline (50 mM Tris-HCl, 150 mM NaCl, 1 mM $MgCl_2$) containing 30 μg of bovine brain calmodulin (Sigma, St. Louis, MO) and either 1 mM $CaCl_2$ or 5 mM ethylene glycol bis(β-aminoethyl ether)-*N*,*N*,*N*′,*N*′-tetraacetic acid (EGTA). The pH of each solution was adjusted to 7.4. The samples were then incubated at 4 °C for 4 h. Following incubation, each sample was washed in the binding solution containing 0.05% polyoxyethylene sorbitan monolaurate (Tween 20, Bio-Rad Laboratories, Hercules, CA). Thereafter, bound protein was eluted with 2% sodium dodecyl sulfate (SDS) sample buffer. The concentration of GST fusion protein in each eluate was first estimated by 11% SDS−polyacrylamide gel electrophoresis using Coomassie Blue stain to equalize loading of GST fusion proteins in subsequent stages of the experiments. Western blotting was then carried out to assay the amount of calmodulin that had previously bound to each GST fusion protein. For this procedure, the eluted products that contained both GST fusion proteins and calmodulin were separated on 11% SDS−polyacrylamide gels. The gels were blotted onto nitrocellulose and incubated with 2 μg/mL mouse anti-calmodulin monoclonal IgG_1 (Upstate Biotechnology, Lake Placid, NY). Each membrane was washed with phosphate-buffered saline containing 0.03% Tween 20 and then incubated with sheep anti-mouse Ig conjugated with horseradish peroxidase (Amersham Pharmacia Biotech). The membranes were then visualized by chemiluminescence (ECL, Amersham Pharmacia Biotech). The same membranes were stained with Ponceau S as a sensitive determination of the relative amount of GST fusion protein in each reaction.

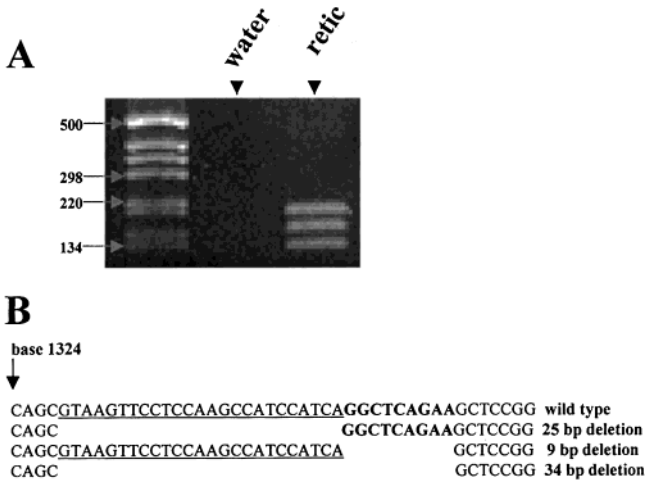

FIGURE 1: Sequences of hSK1 isoforms isolated by RT-PCR. (A) Nested PCR of the region containing deletions. Shown is a 2% agarose gel of the RT-PCR products obtained. (B) Sequences of four variants cloned from nested PCR products.

Peptides that encompassed the variable regions of hSK1, hSK1^{-9b}, and hSK1^{-34b} were synthesized by the Baylor Core Facility for Peptide Synthesis (Table 1). Each peptide was then incubated for 30 min at room temperature with bovine brain calmodulin at varying molar ratios as indicated in Figure 4B. Each reaction mixture contained either 2 mM $CaCl_2$ or 5 mM EGTA. The reaction mixtures were buffered to pH 7.4 with 3-(*N*-morpholino)propanesulfonic acid. The reaction products were resolved on nondenaturing 20% polyacrylamide gels by electrophoresis. The gels were stained by Coomassie Blue dye.

RESULTS

To clone the full-length coding region of the erythroid SK1 channel, we designed oligonucleotide primers from the published sequence of hSK1 (GenBank U69883) (*5*) that allowed us to amplify a series of overlapping fragments. For this purpose, RT-PCR was carried out using RNA from reticulocytes or from *Dami* cells. In the course of these experiments, we noted that amplification of the C-terminal region from either source of RNA yielded products whose direct sequences were ambiguous. Nested PCR permitted the

Table 2: Oligonucleotide PCR Primers

name	position	sequence[a]
hSK1-del sense	1267−1286	5′-ATCTACAAACATACCAGGCT-3′
hSK1-del α-sense	1413−1432	5′-TCTTGGCTAGGTCGGTAAGC-3′
hSK1-RPA sense	965−984	5′-GCGAGAGGTACCACGACAAG-3′
hSK1-CTERM sense	1156−1175	5′-CTGATCGAATTCAAGCTGGAGCTCACCAAGGC-3′ [b]
hSK1-CTERM α-sense	1669−1686	5′-CTATTAACTCGAGTCACCCGCAGTCCGAGGG-3′

[a] Based on the sequence of hSK1 (GenBank U69883). [b] Underlined sequence is linker containing added restriction enzyme site.

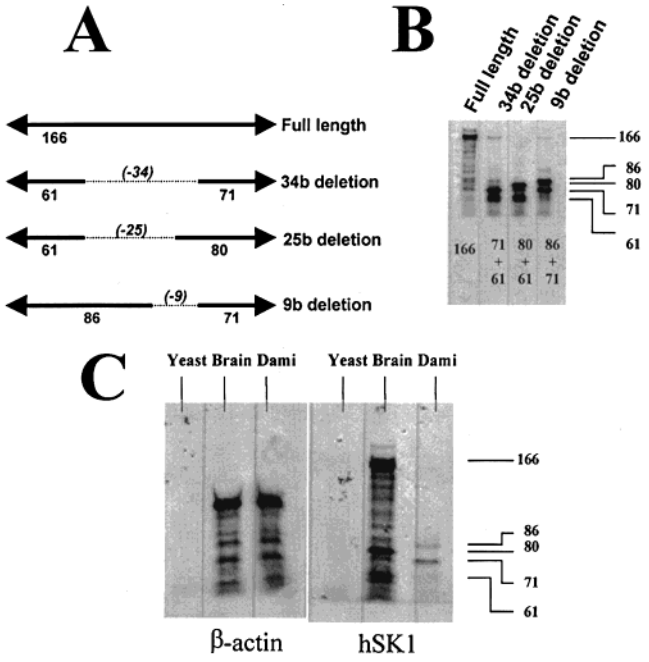

FIGURE 2: Confirmation of existence of mRNA encoding each hSK1 isoform by means of ribonuclease protection assays. (A) Fragment lengths of riboprobe predicted to be protected from RNase digestion by mRNA encoding each isoform. (B) Protection of the riboprobe with RNA transcribed from individual cloned isoforms confirms predictions shown in panel A. (C) Protection of β-actin or hSK1 riboprobes with total yeast RNA or mRNA isolated from the hippocampal region of human brain or from *Dami* cells.

resolution of multiple distinct bands within this region (Figure 1A). To focus on this portion of the coding sequence, we used the oligonucleotide primers hSK1-del sense and hSK1-del α-sense (Table 2). Following amplification by RT-PCR, the DNA products obtained were cloned. By sequencing multiple clones, four variations were consistently observed. These derived from the inclusion or deletion of two adjacent nucleotide sequences that extended 25 and 9 bases in length, respectively (Figure 1B).

To determine the relative proportion of mRNA coding for each of the four variants in hippocampus, reticulocytes, and *Dami* cells, we amplified this region by RT-PCR using mRNA from *Dami* cells and human hippocampus and total RNA from reticulocytes. The DNA products in each case were then cloned. Ninety-one individual clones derived from hippocampal mRNA, 114 from *Dami* cell mRNA, and 74 from reticulocyte RNA were isolated and characterized by restriction digestion or by sequencing. By this approach, we obtained an estimate of the relative ratios of each of the four variants expressed in these tissues. The distribution of the four variants was different in each case. Among the clones derived from hippocampal mRNA, 97% comprised clones of either the full-length variant or hSK1^{-25b}; specifically, the full-length variant accounted for 62%, hSK1^{-25b} for 35%, hSK1^{-34b} for only 3%, and hSK1^{-9b} for none. Among the clones obtained from *Dami* cell mRNA, hSK1^{-9b} comprised 40%, hSK1^{-34b} 31%, hSK1^{-25b} 15%, and the full-length variant only 14%. Among the clones derived from reticulocyte RNA, hSK1^{-34b} were most abundant at 49%, while the full-length variant accounted for 37%, hSK1^{-25b} for 9%, and hSK1^{-9b} for only 4%.

We then used the ribonuclease protection assay to confirm that separate species of mRNA existed for each of the hSK1 variants and that each species was present in *Dami* cells and hippocampus in approximately the same ratios that we had determined by RT-PCR. We hypothesized that the radiolabeled riboprobe that we designed for these experiments would be fully protected by mRNA encoding the undeleted form of hSK1 but would be cleaved into two fragments if it

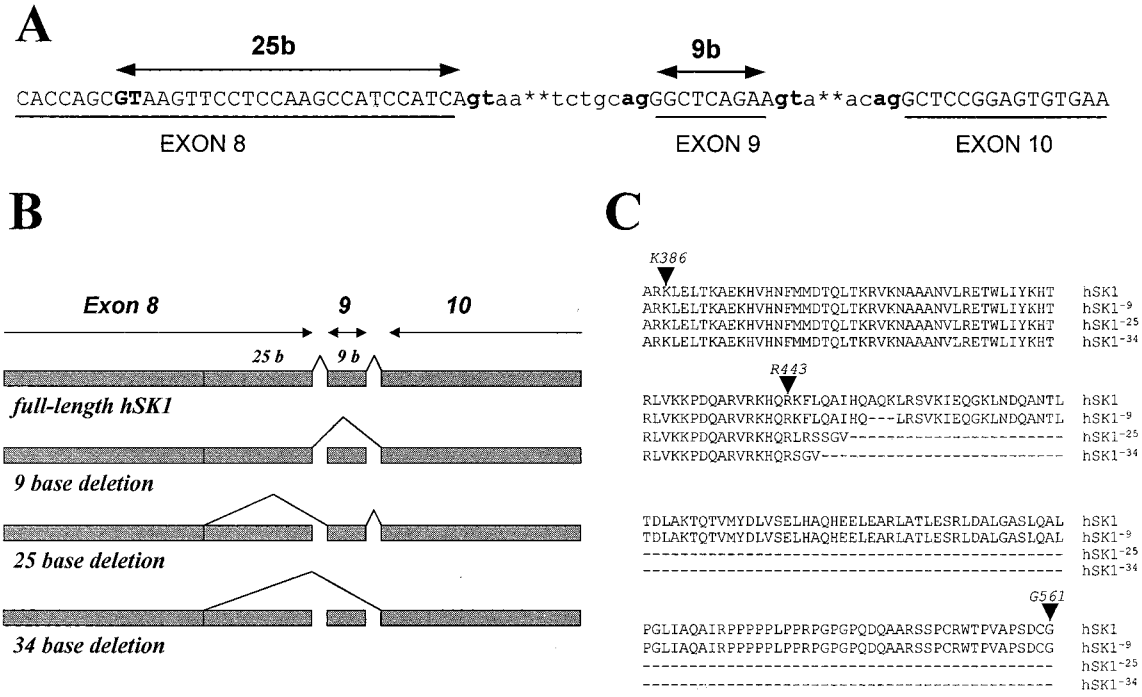

FIGURE 3: Genomic sequencing of hSK1 within the region of the C-terminal deletions. (A) Genomic sequence including 25-base and 9-base stretches flanked by splice donor (GT) and acceptor (AG) sequences. (B) Map of alternative splicing sites. (C) Amino acid sequences predicted for the spliced regions of the C-termini of all four isoforms. GST fusion constructs begin with K386. The sequences of all four hSK1 isoforms are identical through R443.

annealed to mRNA containing either or both of the deletions within the region of the probe. As illustrated in Figure 2A, we predicted that the undeleted variant of hSK1 would yield a single product of 166 bases, that the 34-base deletion would permit 34 bases to be digested from the probe and the two flanking regions (of 61 bases and 71 bases, respectively) to be protected, that the 25-base deletion would protect the two flanking regions of 61 bases and 80 bases, and that a 9-base deletion would yield two products of 86 bases and 71 bases. We prepared individual clones of each of the four variants of hSK1 in order to determine whether this plan was sound. We then transcribed mRNA from each of these clones and allowed each sample to react with the radiolabeled riboprobe. As shown in Figure 2B, fragments of the predicted length were obtained in every case. We then used this approach to test whether the individual mRNA species were expressed in the ratios that we had predicted in *Dami* cells and in hippocampus. On the basis of the percentages of each variant that we had found, we expected that more of the fully protected 166-base riboprobe would result from its incubation with hippocampal mRNA than with *Dami* cell mRNA. Furthermore, we predicted that the two most abundant fragments that would result from incubation of the probe with *Dami* cell mRNA would be one 71 bases long, since fragments of that length would be produced by both the 9-base and the 34-base deletion, and another 86 bases long, because of the predicted abundance of the 9-base deletion in *Dami* cells. As illustrated in Figure 2C, the results that we obtained confirmed these predictions. Although equal quantities of *Dami* cell and hippocampal mRNA were used in each experiment, the fact that the signals for each hSK1 fragment were much stronger from hippocampal mRNA indicates that the amount of hSK1 mRNA was substantially greater in hippocampus than in *Dami* cells.

Using *Dami* cell DNA, we then carried out genomic sequencing of the region encompassing the deletions. By this approach, we found that each of the isoforms that we had identified could be accounted for by alternative splicing of a single hSK1 gene (Figure 3). The 25-base deletion began with a splice donor site within exon 8 (*20*) and extended to the downstream end of the exon. The nine-base deletion, which was bounded bilaterally by intron sequences, composed the entirety of exon 9. Donor (GT) and acceptor (AG) splicing sites were identified which permitted the construction of each of the four isoforms.

The amino acid sequences predicted for each of the four isoforms are illustrated in Figure 3C. Deletion of either 25 bases (hSK1^{-25b}) or 34 bases (hSK1^{-34b}) results in out-of-frame mutations that give rise in each case to the removal of the terminal 118 amino acids. In hSK1^{-25b}, six amino acids (LRSSGV) are added to the truncated C-terminus before a stop codon is encountered, and in hSK1^{-34b}, three new amino acids (SGV) are encoded. In the nine-base deletion (hSK1^{-9b}), only the three amino acids A452, Q453, and K454 are removed. Although this nine-base deletion is out of frame, the remainder of the C-terminus is intact.

To determine whether the alterations introduced into the C-terminus of hSK1 by alternative splicing affected calmodulin binding, we used two approaches. First, we constructed GST fusion proteins containing the cytoplasmic C-terminus of each splice variant and tested their ability to bind to calmodulin in the presence or absence of Ca^{2+} ions.

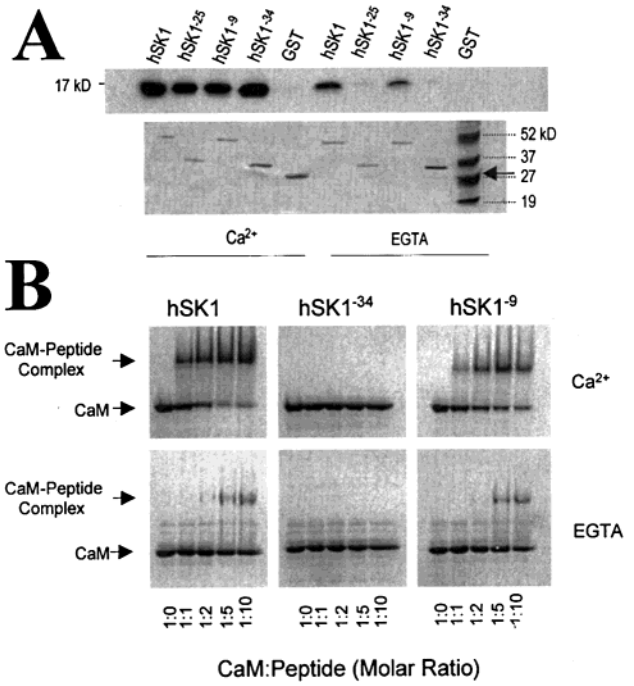

FIGURE 4: Calmodulin binding to C-termini of hSK1 splice variants. (A) GST pull-down assays of calmodulin binding to the cytoplasmic C-termini of hSK1 splice variants. In the top panel, calmodulin that bound to each GST fusion protein or to GST alone in the presence of Ca^{2+} or EGTA was detected by western blotting using an anti-calmodulin antibody (17 kDa). The loading volume in each lane varied between 18 and 30 μL in order to equalize the amount of GST fusion proteins in each reaction (see Experimental Procedures). In the lower panel, the same membrane was stained with Ponceau S to permit estimation of protein loading (GST, 29 kDa; hSK1 and hSK1^{-9b}, ~50 kDa; and hSK1^{-34b} and hSK1^{-25b}, ~37 kDa). In the lane farthest to the right, in which GST and molecular weight markers were superimposed, the 29 kDa GST band is marked by the arrow. (B) Gel-shift assays of the binding affinity of calmodulin to synthetic hSK1 peptides on nondenaturing gels. Peptides based on the C-terminal sequences of hSK1, hSK1^{-34b}, and hSK1^{-9b} (Table 1) were incubated with calmodulin at different molar ratios in the presence of Ca^{2+} or EGTA. Each reaction contained 296 pmol of calmodulin and 0−2.96 nmol of peptide, yielding ratios between 1:0 and 1:10. Free calmodulin (CaM) was then distinguished from calmodulin bound to hSK1 peptides (CaM−peptide complex) by electrophoresis on native gels.

As shown in Figure 4A, we found that calmodulin bound strongly to all four fusion proteins in the presence of Ca^{2+}. In the absence of Ca^{2+}, calmodulin binding was generally diminished. However, the binding of calmodulin to the truncation variants hSK1^{-25b} and hSK1^{-34b} was markedly diminished under these conditions when compared to hSK1, although binding to hSK1^{-9b} was not substantially affected.

We then synthesized oligopeptides that encompassed the affected regions of hSK1, hSK1^{-9b}, and hSK1^{-34b} (Table 1). These peptides were assessed for their ability to bind calmodulin in gel-shift assays. As shown in Figure 4B, calmodulin bound equally well to hSK1 and hSK1^{-9b} peptides. In each case, binding was greater in the presence of Ca^{2+} ions. In contrast, no binding of calmodulin to the hSK1^{-34b} peptide was detected either with or without Ca^{2+}.

DISCUSSION

Our studies in human erythroid cells indicate that at least four isoforms of hSK1 exist whose structures differ from one another in the amino acid sequences of their C-terminal

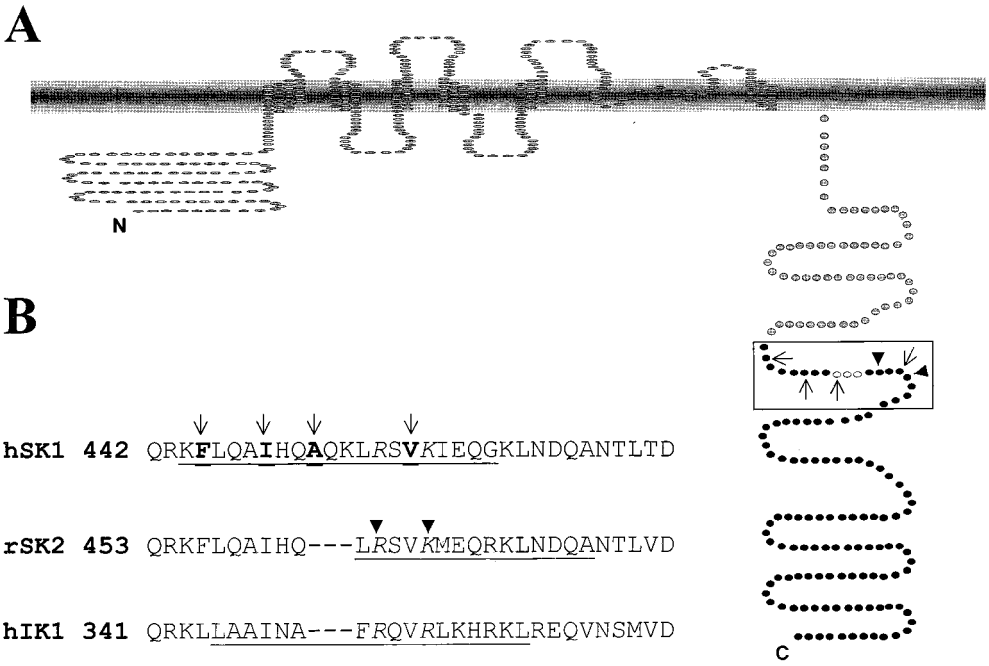

FIGURE 5: Calmodulin binding domains in SK/IK channels. (A) Model of hSK1. A452, Q453, and K454, which are deleted in $hSK1^{-9b}$, are indicated by white circles. The 118 terminal amino acids deleted in the truncated variants $hSK1^{-25b}$ and $hSK1^{-34b}$ are shown as black circles. The 20 amino acid sequence that we found by gel-shift assays (Figure 4) to bind both apocalmodulin and Ca^{2+}-calmodulin is enclosed by the square. The 1−8−14 Ca^{2+}-calmodulin binding motif present in hSK1 is designated by arrows, and the two positively charged amino acids (R456 and K459) corresponding to those found by Keen et al. (*9*) to be necessary for apocalmodulin binding in rSK2 are highlighted by black triangles. (B) Sequences of the mid-region of C-termini of SK and IK channels implicated in calmodulin binding. The numbers refer to the positions within their respective coding frames of the amino acids that begin each sequence. hSK1: The 20 amino acid sequence that we found to bind both apocalmodulin and Ca^{2+}-calmodulin in hSK1 is underlined, and the 1−8−14 Ca^{2+}-calmodulin binding motif is emboldened and designated by arrows. rSK2: A 15 amino acid sequence determined by Xia et al. (*7*) to be crucial for Ca^{2+} gating in rSK2 is underlined. The two positively charged amino acids found by Keen et al. (*9*) to be necessary for apocalmodulin binding in rSK2 (R464 and K467) are shown in italics and highlighted by black triangles, and the corresponding residues in the other sequences are indicated in italics. hIK1: A region reported by Fanger et al. (*10*) to be important in Ca^{2+}-calmodulin binding in hIK1 is underlined.

cytosolic domains. The three deletion variants of the native hSK1 pore-forming subunit $hSK1^{-9b}$, $hSK1^{-25b}$, and $hSK1^{-34b}$ result from alternative splicing of mRNA transcribed by a single hSK1 gene. In $hSK1^{-9b}$, a deletion of three amino acids is introduced in the middle of the cytoplasmic tail of the protein, while in both $hSK1^{-25b}$ and $hSK1^{-34b}$, over half of the cytoplasmic region of the C-terminus is deleted. The relative distribution of each of the four isoforms in erythropoietic tissue is different from that in the hippocampal region of human brain, in which the full-length variant predominates. $hSK1^{-34b}$ is the major species in reticulocytes, while $hSK1^{-9b}$ is prevalent in *Dami* leukemia cells in culture. Our findings indicate that as is the case with large conductance Ca^{2+}-activated K^+ (BK) channels (*22*), alternative splicing may be a mechanism through which the diversity of the function of SK/IK channels has been amplified. Since calmodulin binding to the truncated variants $hSK1^{-25b}$ and $hSK1^{-34b}$ is diminished in comparison to hSK1 and $hSK1^{-9b}$, our results predict that the sensitivity of tetrameric K^+ channels assembled from various combinations of these subunits may be altered.

The precise sites on SK and IK channels to which calmodulin binds are unclear. Through studies on rSK2, Xia et al. (*7*) proposed that calmodulin was bound within a shell formed by the four α-helices of the C-terminus and that different binding sites existed for apocalmodulin and Ca^{2+}-calmodulin. By expression of a series of truncation mutants of SK2, they were able to localize a region of 15 amino acids that was essential for Ca^{2+} gating (Figure 5). Recently, Keen et al. (*9*) found that the same region of SK2 functioned in apocalmodulin binding, since two positively charged amino acids (R464 and K467) within this domain were essential for the binding of calmodulin in the absence of Ca^{2+} ions (Figure 5). In hSK1, the corresponding residues (R456 and K459) lie immediately downstream from the three amino acids deleted in $hSK1^{-9b}$ (A452, Q453, and K454). In both $hSK1^{-25b}$ and $hSK1^{-34b}$, these amino acids are eliminated. Our finding that a 20-amino acid sequence from this region of hSK1, or the corresponding 17 residues from $hSK1^{-9b}$, permitted calmodulin binding both in the presence and in the absence of Ca^{2+} ions (Figure 4A) corroborates the observations of Xia et al. and Keen et al. and underscores the importance of this relatively small region of the C-terminus in both apocalmodulin and Ca^{2+}-calmodulin binding.

Fanger et al. (*10*) and Khanna et al. (*8*) have recently observed that different regions of the C-terminus of hIK1 also exhibit different binding affinities for apocalmodulin or Ca^{2+}-calmodulin. The calmodulin-binding domains mapped by Fanger et al. in hIK1 appear generally to correspond to the regions of rSK2 and hSK1 that participate in both apocalmodulin and Ca^{2+}-calmodulin binding (Figure 5). In addition, Khanna et al. reported that deletion of the distal half of the C-terminus diminishes the binding of apocalmodulin but not Ca^{2+}-calmodulin binding. Their observation is remarkably similar to our finding that deletion of the distal 118 amino acids of the C-terminus in $hSK1^{-25b}$ and $hSK1^{-34b}$ eliminates apocalmodulin binding but leaves Ca^{2+}-calmodulin binding practically intact.

When our findings in hSK1 are considered together with those of Xia et al. (*7*) and Keen et al. (*9*) in rSK2 and those of Fanger et al. (*10*) and Khanna et al. (*8*) in hIK1, a view of calmodulin binding to SK and IK channels emerges in which large portions of the C-terminus are probably involved in apocalmodulin binding, while Ca^{2+}-calmodulin may bind to a more restricted region in the middle of the cytoplasmic C-terminal tail. Our experiments establish that a sequence of 20 amino acids in this region of hSK1 or the corresponding 17 amino acid sequence in $hSK1^{-9b}$, which are jettisoned in the truncated splice variants $hSK1^{-25b}$ and $hSK1^{-34b}$, exhibit both apocalmodulin and Ca^{2+}-calmodulin binding properties. The alternative splicing of hSK1 that we have described permitted a natural confirmation of much of the calmodulin binding data that were obtained in rSK2 (*7*, *9*) and hIK1 (*8*, *10*) through a series of engineered deletions.

The effects of second messengers other than calmodulin may be modified by the deletions introduced into the C-terminus through alternative splicing. The terminal 118 amino acids deleted in the truncated variants $hSK1^{-25b}$ and $hSK1^{-34b}$ contain two casein kinase II phosphorylation domains, two leucine zipper motifs, and one protein kinase C phosphorylation site. Although casein kinase II has not been reported to affect the gating of K^+ channels, its potential effect on SK channels cannot be discounted since phosphorylation by this kinase has been implicated in the regulation of both NMDA (*23*) and ryanodine receptors (*24*). And while protein kinase C has not been reported to date to regulate SK channels, it has been proposed to affect the gating of several other kinds of K^+channels, including BK (*25*) and IK (*26*) channels.

The deletion of the three amino acids A452, Q453, and K454 in $hSK1^{-9b}$ does not appear either to disrupt any of the phosphorylation or binding sites described above or to unmask new consensus domains for other signaling molecules. It is of considerable interest, however, that although these three amino acids are present in hSK1 and its orthologue rSK1, they are absent from other members of the SK/IK family of Ca^{2+}-activated K^+ channels (*2*−*5*).

ACKNOWLEDGMENT

The authors thank Drs. Susan Hamilton and Jia-Zheng Zhang for their generous help in the nondenaturing gel assays of calmodulin binding and Drs. Jorge Sepulveda and Hua Chen for many helpful discussions.

REFERENCES

1. Wallner, M., Meera, P., and Toro, L. (1999) in *Calcium-activated potassium channels in muscle and brain* (Kurachi, Y., Jan, L. Y., and Lazdunski, M., Eds.) Vol. 8, pp 117−140.
2. Ishii, T. M., Silvia, C., Hirschberg, B., Bond, C. T., Adelman, J. P., and Maylie, J. (1997) *Proc. Natl. Acad. Sci. U.S.A. 94*, 11651−11656.
3. Joiner, W. J., Wang, L.-Y., Tang, M. D., and Kaczmarek, L. K. (1997) *Proc. Natl. Acad. Sci. U.S.A. 94*, 11013−11018.
4. Logsdon, N. J., Kang, J., Togo, J. A., Christian, E. P., and Aiyar, J. (1997) *J. Biol. Chem. 272*, 32723−32726.
5. Köhler, M., Hirschberg, B., Bond, C. T., Kinzie, J. M., Marrion, N. V., Maylie, J., and Adelman, J. P. (1996) *Science 273*, 1709−1714.
6. Schreiber, M., and Salkoff, L. (1997) *Biophys. J. 73*, 1355−1363.
7. Xia, X. M., Fakler, B., Rivard, A., Wayman, G., Johnson-Pais, T., Keen, J. E., Ishii, T., Hirschberg, B., Bond, C. T., Lutsenko, S., Maylie, J., and Adelman, J. P. (1998) *Nature 395*, 503−507.
8. Khanna, R., Chang, M. C., Joiner, W. J., Kaczmarek, L. K., and Schlichter, L. C. (1999) *J. Biol. Chem. 274*, 14838−14849.
9. Keen, J. E., Khawaled, R., Farrens, D. L., Neelands, T., Rivard, A., Bond, C. T., Janowsky, A., Fakler, B., Adelman, J. P., and Maylie, J. (1999) *J. Neurosci. 19*, 8830−8838.
10. Fanger, C. M., Ghanshani, S., Logsdon, N. J., Rauer, H., Kalman, K., Zhou, J., Beckingham, K., Chandy, K. G., Calahan, M. D., and Aiyar, J. (1999) *J. Biol. Chem. 274*, 5746−5754.
11. Grygorczyk, R., and Schwarz, W. (1983) *Cell Calcium 4*, 499−510.
12. Wolff, D., Cecchi, X., Spalvins, A., and Canessa, M. (1988) *J. Membr. Biol. 106*, 243−252.
13. Dunn, P. M. (1998) *J. Membr. Biol. 165*, 133−143.
14. Christophersen, P. (1991) *J. Membr. Biol. 119*, 75−83.
15. Romero, P. J., and Rojas, L. (1992) *Acta Cient. Venez. 43*, 19−25.
16. Rhoads, A. R., and Friedberg, F. (1997) *FASEB J. 11*, 331−340.
17. Beutler, E., West, C., and Blume, K. G. (1976) *J. Lab. Clin. Med. 88*, 328−333.
18. Murphy, J. R. (1973) *J. Lab. Clin. Med. 82*, 334−341.
19. Sullivan, R., Kunze, D. L., and Kroll, M. H. (1996) *Blood 87*, 648−656.
20. Litt, M., LaMorticella, D., Bond, C. T., and Adelman, J. P. (1999) *Cytogenet. Cell. Genet. 86*, 70−73.
21. Frangioni, J. V., and Neel, B. G. (1993) *Anal. Biochem. 210*, 179−187.
22. Tseng-Crank, J., Foster, C. D., Krause, J. D., Mertz, R., Godinot, N., DiChiara, T. J., and Reinhart, P. H. (1994) *Neuron 13*, 189−193.
23. Lieberman, D. N., and Mody, I. (1999) *Nat. Neurosci. 2*, 125−132.
24. Shoshan-Barmatz, V., Orr, I., Weil, S., Meyer, H., Varsanyi, M., and Heilmeyer, L. M. (1996) *Biochim. Biophys. Acta 1283*, 89−100.
25. Ribalet, B., and Eddlestone, G. T. (1995) *J. Membr. Biol. 148*, 111−125.
26. Rivera, A., Rotter, M. A., and Brugnara, C. (1999) *Am. J. Physiol. 277*, C746−C754.

BI001675H